PRAMANA
— journal of
physics

Vol. 70, No. 2
February 2008
pp. 313–321

Re-dispersible Li^+ and Eu^{3+} co-doped CdS nanoparticles: Luminescence studies

N S GAJBHIYE[1], RAGHUMANI SINGH NINGTHOUJAM[2,*], ASAR AHMED[1], D K PANDA[1], S S UMARE[3] and S J SHARMA[4]

[1]Department of Chemistry, Indian Institute of Technology, Kanpur 208 016, India
[2]Chemistry Division, Bhabha Atomic Research Centre, Mumbai 400 085, India
[3]Department of Chemistry, Visvesvaraya National Institute of Technology, Nagpur 440 011, India
[4]Department of Electronics, S.K. Porwal College, Kamptee, Nagpur 441 002, India
*Corresponding author. E-mail: rsn@barc.gov.in; nsg@iitk.ac.in

Abstract. Re-dispersible CdS, 5 at.% Eu^{3+}-doped CdS, 2 at.% Li^+ and 5 at.% Eu^{3+} co-doped CdS nanoparticles in organic solvent are prepared by urea hydrolysis in ethylene glycol medium at a low temperature of 170°C. CdS nanoparticles have spherical shape with a diameter of ∼80 nm. The asymmetric ratio (A_{21}) of the integrated intensities of the electrical dipole transition to the magnetic dipole transition for 5 at.% Eu^{3+}-doped CdS is found to be 3.8 and this ratio is significantly decreased for 2 at.% Li^+ and 5 at.% Eu^{3+} co-doped CdS ($A_{21} = 2.6$). It establishes that the symmetry environment of Eu^{3+} ion is more favored by Li-doping. Extra peak at 550 nm (green emission) could be seen for 2 and 5 at.% Eu^{3+} co-doped CdS. Also, the significant energy transfer from host CdS to Eu^{3+} is found for 5 at.% Eu^{3+}-doped CdS compared to that for 2 at.% Li^+ and 5 at.% Eu^{3+} co-doped CdS.

Keywords. Semiconductor; luminescence; lanthanide ions; nanoparticles; re-dispersible.

PACS Nos 61.72.w; 61.46.Df; 81.20.Rg; 78.55.Qr; 76.30.Kg

1. Introduction

Studies on the electronic and optical properties of semiconductor spherical quantum dots are important for various potential applications afforded by their size-dependent band gap and exciton spectra, such as solar cells, lasers, and fluorescent tags in biotechnology applications [1–5]. Cadmium sulfide, a semiconductor with a band gap of 2.4 eV, is an interesting material for optoelectronic device applications. In particular, *n*-type CdS is used to form heterojunctions with *p*-CdTe and other chalcopyrite thin films for its implementation in low-cost and high efficiency solar cells. Many works on luminescence of CdS nanoparticles were reported. In order to improve luminescence properties of CdS nanoparticles, lanthanide ions like Eu^{3+} could be incorporated. Eu^{3+} can substitute Cd^{2+} because of similar ionic radii,

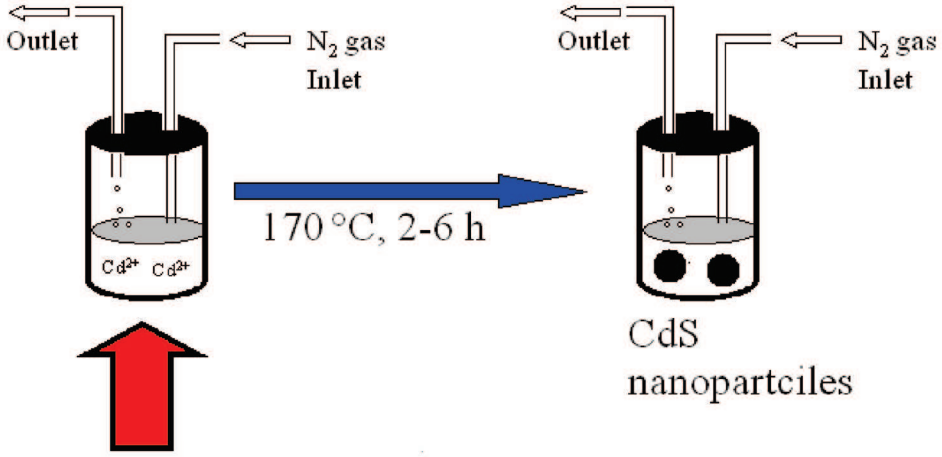

Figure 1. The schematic diagram of the preparation of CdS nanoparticles from ethylene glycol medium in N_2 gas atmosphere at 170°C for 3 h and thiourea is used as a source of S^{2-} ions during reaction.

i.e., ionic radii of Eu^{3+} and Cd^{2+} are 0.94 and 0.97 Å respectively. But positive charges in both are not same. To compensate charge balance, it is needed to add a positive ion such as Li^+, Na^+ and K^+. Li^+ has high diffusivity and low activation energy because of its small ionic radius (0.59 Å). Studies of Li^+ and Eu^{3+} co-doped in CdS have not been widely reported. But there have been reports in the literature regarding the enhancement of luminescence intensity by Li^+ and Eu^{3+} co-doping in other semiconducting materials [4–6]. Some reports of Eu^{3+}-doped CdS nanoparticles are also available in literatures [7–10]. However, energy transfer between CdS host and Eu^{3+} ions is not mentioned much. Another challenge is the preparation of materials, which can be re-dispersible in organic solvent at room temperature. Such materials can be incorporated in polymer-based materials and optical fibres [11,12]. Also, it can be used as sensor for drug delivery in our body [12,13].

In the present work, we prepare re-dispersible CdS, Li^+- and Eu^{3+}-doped CdS nanoparticles in organic solvent by urea hydrolysis at 170°C and their luminescence properties are studied. We propose the mechanism of re-dispersion of CdS nanoparticles in organic solvent.

2. Experimental section

For the preparation of CdS, 10 ml of 0.1 M cadmium sulfate is mixed with 2 g of thiourea in a two-necked round bottom flask. Fifty milliliters of ethylene glycol is added into it. It is refluxed at 170°C for 3 h in N_2 atmosphere. A yellow precipitate appears and is collected using centrifugation. To remove excess ethylene glycol, it is again centrifuged by adding methanol and acetone. Also, 5 at.% Eu^{3+}-doped CdS (Eu^{3+}-doped CdS), and 2 at.% Li^+ and 5 at.% Eu^{3+} co-doped CdS (Li^+ and Eu^{3+} co-doped CdS) particles are prepared by similar method. Sources of Li^+ and Eu^{3+}

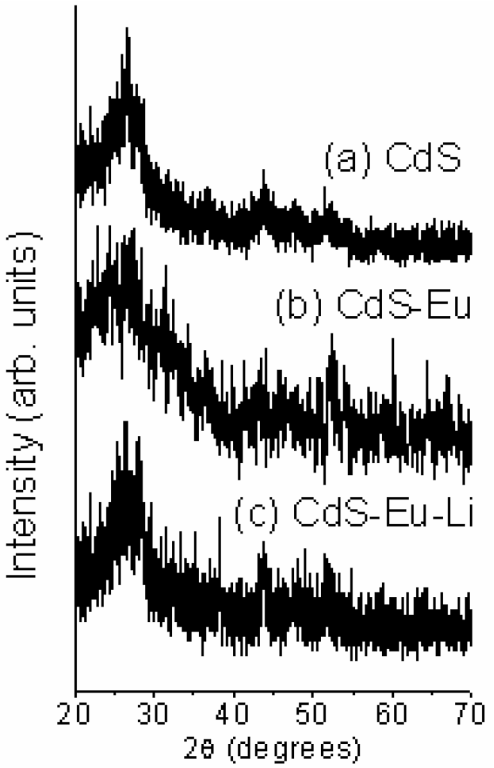

Figure 2. XRD patterns of as-prepared (**a**) CdS and (**b**) Eu^{3+}-doped CdS and (**c**) Li^+ and Eu^{3+} co-doped CdS.

are Li-acetate and Eu_2O_3 respectively. The schematic diagram of the preparation of CdS nanoparticles from ethylene glycol medium in N_2 gas atmosphere at 170°C for 3 h and thiourea is used as a source of S^{2-} ions during reaction (figure 1).

The powder X-ray diffraction (XRD) patterns of the CdS and Li^+- and Eu^{3+}-doped CdS samples are recorded with Cu K_α radiation and Ni-filter in the 2θ range 35–120° using a Rich Seifert Isodebyflex X-ray unit model 2002. The average crystallite size (t) is calculated from the line broadening using the Scherrer's relation: $t = 0.9\lambda/B\cos\theta$, where λ is the wavelength of X-rays and B is the half maximum linewidth. Scanning electron microscope (SEM), JEOL JSM-840A is used to investigate the particle size distribution and morphology. Luminescence measurements are performed using Fluorolog (R)-3 Spectrofluorometer. Powder samples are spread over a quartz plate and mounted inside the sample chamber.

3. Results and discussion

Figures 2a–c show XRD patterns of as-prepared CdS, Eu^{3+}-doped CdS and Li^+ and Eu^{3+} co-doped CdS. The X-ray diffraction studies on nanoparticles of CdS,

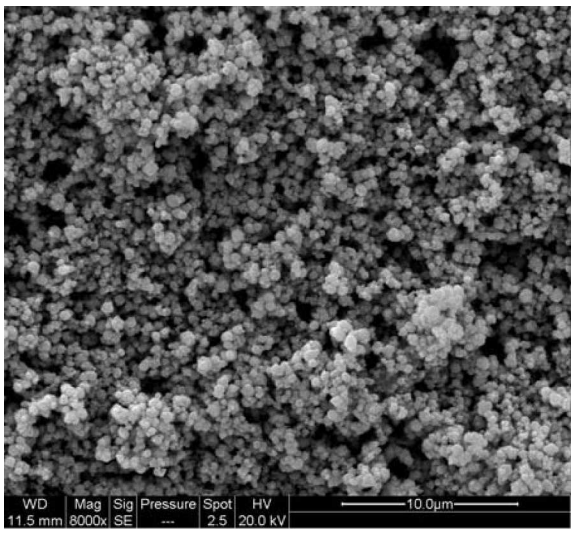

Figure 3. SEM image of CdS nanoparticles.

Eu^{3+}-doped CdS and Li^{+} and Eu^{3+} co-doped CdS show that they are crystalline and show cubic structure (JCPDS 42-1411). Lattice parameter (a) for CdS is found to be 5.84 Å. However, exact calculation of lattice parameter is difficult as peaks in XRD pattern are broad. The average crystallite sizes for CdS, Eu^{3+}-doped CdS and Li^{+} and Eu^{3+} co-doped CdS are calculated from the highest peak in XRD pattern using Scherrer's relation, and found to be 1.6, 2.0 and 1.5 nm respectively.

Figure 3 shows SEM image of CdS nanoparticles. It gives spherical shape of 80 nm. Particles are well-distributed homogeneously. However, particle size determined by SEM is more than that of XRD. It indicates that a particle has the agglomeration of nanocrystals.

Figure 4 shows photoluminescence (PL) spectra of as-prepared CdS at two different excitations 350 and 394 nm. At 350 nm excitation, major emission peaks at 417, 444 and 532 nm are observed. The peaks at ∼417–444 nm and 532 nm are due to the band–band and lattice defect emission respectively [14–18]. At 394 nm excitation, only one peak at 532 nm is observed, but intensity of the peak is very weak compared to that at 350 nm excitation.

Figure 5 shows the excitation spectrum of 5 at.% Eu^{3+}-doped CdS nanoparticles monitored at 615 nm. The prominent peak at 395 nm could be seen and it is due to Eu^{3+} ion ($^7F_0 \rightarrow {}^5L_6$).

Figure 6a shows the emission spectrum of 5 at.% Eu^{3+}-doped CdS nanoparticles on direct excitation of Eu^{3+} at 394 nm. The emission peaks due to Eu^{3+} at 592 and 616 nm could be observed. The peaks at 592 and 616 nm are due to the intra-4f transitions of Eu^{3+} ions and correspond to the magnetic dipole transition, $^5D_0 \rightarrow {}^7F_1$ and the electronic dipole transition, $^5D_0 \rightarrow {}^7F_2$ respectively. Usually, the electronic dipole transition, $^5D_0 \rightarrow {}^7F_2$ is hypersensitive to Eu^{3+} symmetry. Eu^{3+} symmetry could be defined by asymmetric ratio (A_{21}) of the integrated intensities of $^5D_0 \rightarrow {}^7F_2$ to $^5D_0 \rightarrow {}^7F_1$ and A_{21} is found to be 3.6. Here, peak at 530 nm (due

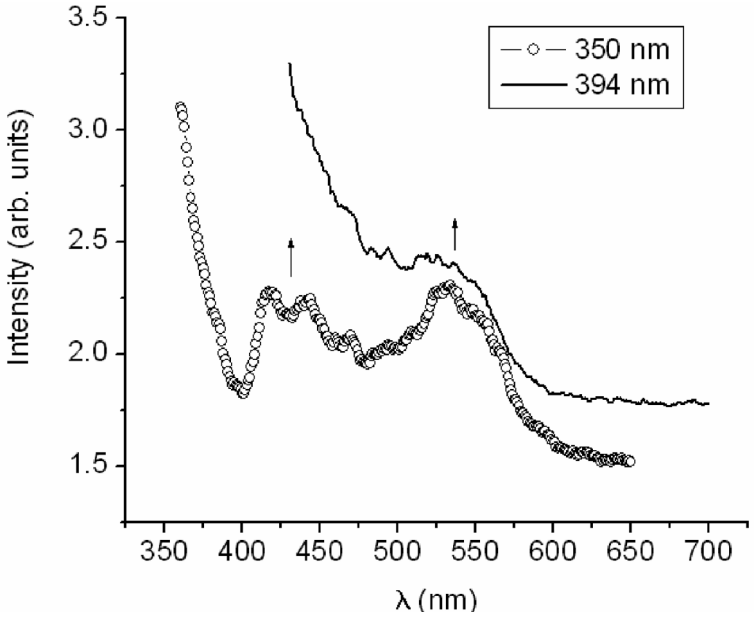

Figure 4. Emission spectra of CdS at different excitations 350 and 394 nm.

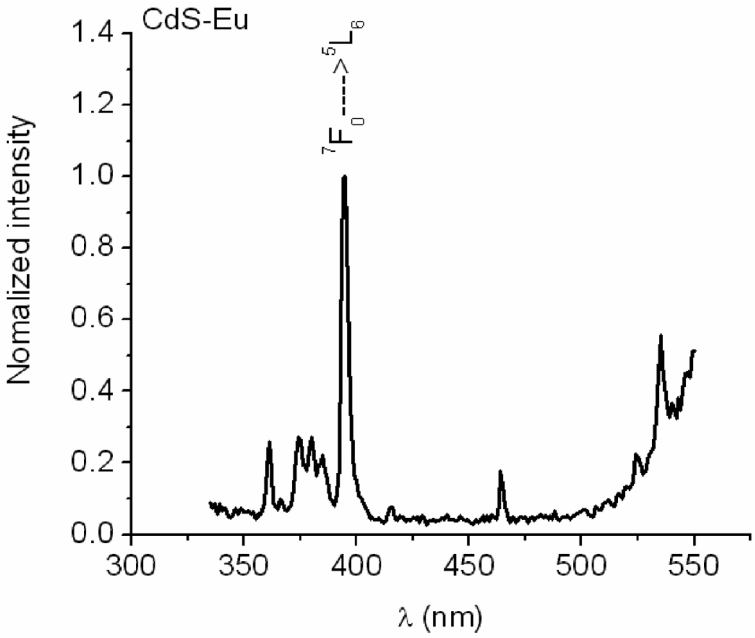

Figure 5. Excitation spectrum of 5 at.% Eu^{3+}-doped CdS nanoparticles at 615 nm emission.

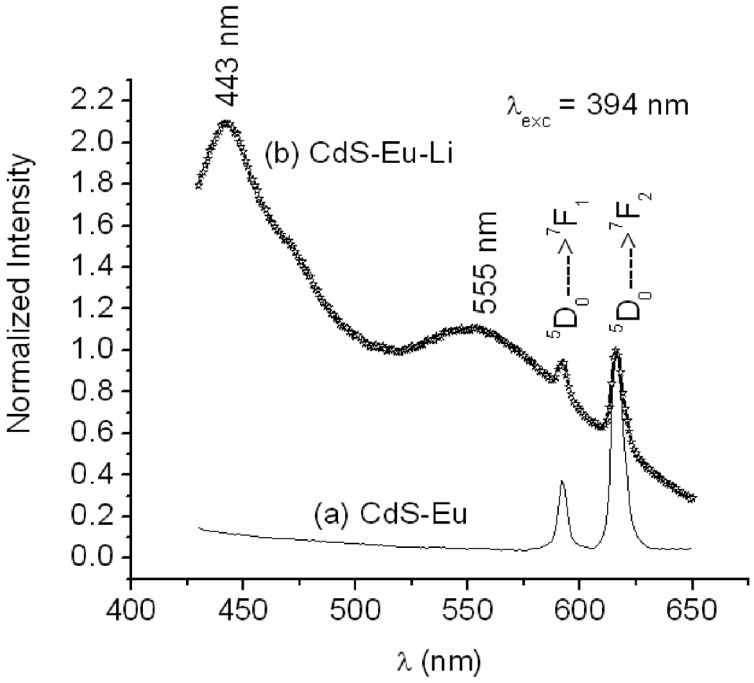

Figure 6. Photoluminescence emission spectra of (**a**) 5 at.% Eu^{3+}-doped CdS and (**b**) 2 at.% Li^{+} and 5 at.% Eu^{3+} co-doped CdS nanoparticles at 394 nm excitation.

to host) could not be observed because its intensity is dominated by intensity from the peaks at 592 and 616 nm.

Figure 6b shows the emission spectrum of 2 at.% Li^{+} and 5 at.% Eu^{3+} co-doped CdS nanoparticles at 394 nm excitation. The peaks due to Eu^{3+} at 592 and 616 nm could be observed. A_{21} is found to be 2.6. It suggests that symmetry environment of Eu^{3+} ion is more enhanced by Li-doping compared to that of 5 at.% Eu^{3+}-doped CdS nanoparticles. Interestingly, peaks at 443 and 555 nm are observed and these are due to CdS host. The peak at 443 nm is due to the band–band emission and peak at 555 nm is due to the lattice defect [14–18].

In pure Eu_2O_3, the 340–355 nm and 470–500 nm range do not excite the Eu^{3+} ions [19]. In order to check energy transfer between CdS and Eu^{3+}, 5 at.% Eu^{3+}-doped CdS nanoparticles are excited at 350 nm through CdS host (figure 7a). There is a strong blue emission at 440 nm along with orange emission at 590 nm and red emission at 615 nm. The peak at 440 nm is due to the CdS host and the peaks at 590 and 615 nm are due to the Eu^{3+} ions. This confirms that the energy can be significantly transferred from the host CdS to Eu^{3+}, while, 2 at.% Li and 5 at.% Eu^{3+} co-doped CdS nanoparticles show the emission at 440 and 559 nm (figure 7b). The peaks at 440 and 559 nm are due to the band–band and lattice defect emission from host CdS respectively. There is no peak for Eu^{3+}. This may be due to quenching/overlapping with a broad peak in the range 535–650 nm. Similar

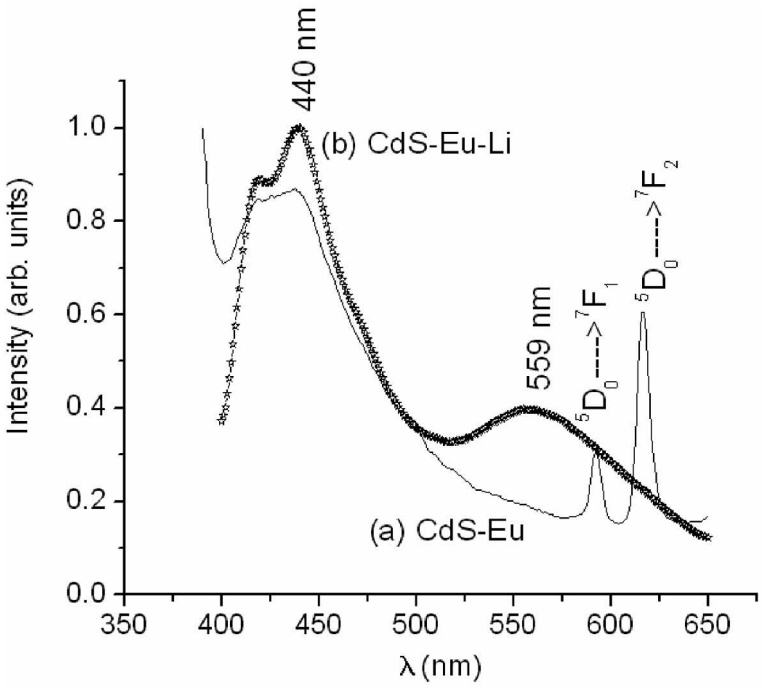

Figure 7. Photoluminescence emission spectra of (**a**) 5 at.% Eu^{3+}-doped CdS and (**b**) 2 at.% Li^+ and 5 at.% Eu^{3+} co-doped CdS nanoparticles at 350 nm excitation.

feature was reported, but peak at 559 nm was not reported in the case of Eu-doped CdS nanoparticles [12,13,20].

The UV absorption study on CdS nanoparticles, which are re-dispersible in ethanol shows absorption at ∼390 nm. IR spectrum of CdS nanoparticles is shown in figure 8. There are O–H, C–H, C–C, C–O functional groups in addition to Cd–S bond. Such extra functional groups are due to incorporation of ethylene glycol molecules, which act as capping. There are two O–H bonds in ethylene glycol molecule. One O–H bond binds with CdS particles. Agglomeration among particles is hindered due to capping. The other O–H bond can interact with methanol or ethanol (organic solvent) through inter-H-bonding. These two O–H bonds are identified in 3000–3400 cm^{-1}. The peak at 3182 cm^{-1} is due to inter H-bonding and the peak at 3294 cm^{-1} is due to O–H bond, which is binding with CdS particles. These materials could be incorporated in polymer-based materials and optical fibres, which may be useful in many applications [21–25]. The proposed mechanism is also shown in figure 9.

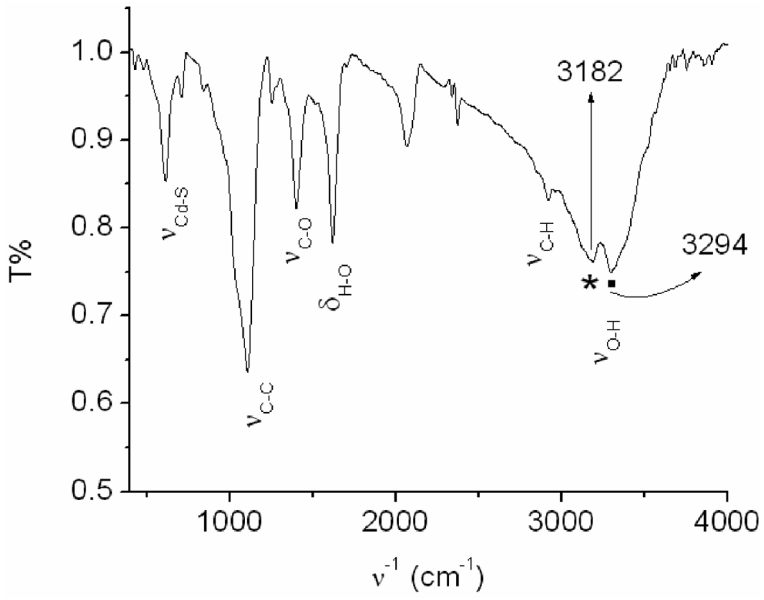

Figure 8. IR spectrum of CdS nanoparticles.

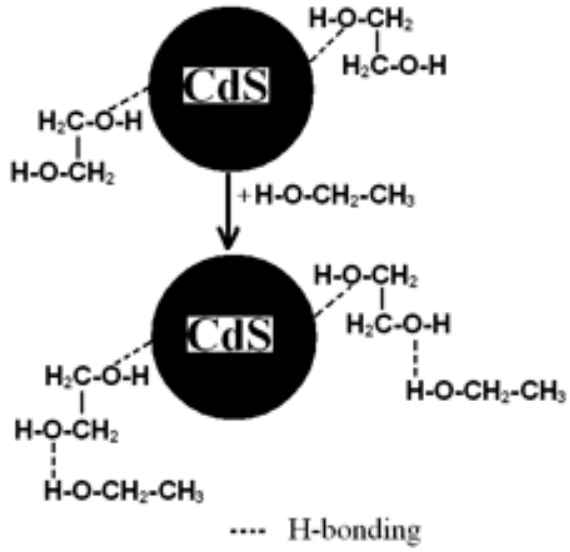

Figure 9. Proposed mechanism for re-dispersible CdS nanoparticles in organic molecules such as methanol and ethanol.

4. Conclusions

CdS, Eu^{3+}-doped CdS, Li^{+} and Eu^{3+} co-doped CdS nanoparticles are prepared and these are re-dispersible in organic solvent. There is a strong energy transfer

from the host CdS to Eu^{3+} ions. Extra peak at 559 nm (green emission) could be seen for 2 at.% Li and 5 at.% Eu^{3+} co-doped CdS.

Acknowledgement

Authors acknowledge the financial support from DST and CSIR, New Delhi.

References

[1] L Yang, Q Shen, J Zhou and K Jiang, *Mater. Chem. Phys.* **98**, 125 (2006)
[2] A P Alivisatos, *J. Phys. Chem.* **B100**, 13226 (1996)
[3] A P Alivisatos, *Science* **271**, 933 (1996)
[4] X Peng, J Wickham and A P Alivisatos, *J. Am. Chem. Soc.* **120**, 5343 (1998)
[5] C B Murray, D J Norris and M G Bawendi, *J. Am. Chem. Soc.* **115**, 706 (1993)
[6] S Tiwari and S Tiwari, *Solar Energy Materials & Solar Cells* **90**, 1621 (2006)
[7] H Zhang, X Fu, S Niu, G Sun and Q Xin, *J. Lumin.* **115**, 7 (2005)
[8] Y Qian, K Hara, H Munekata and H Kukimoto, *Jpn. J. Appl. Phys.* **34**, L368 (1995)
[9] S Bachir, K Azuma, J Kossanyi and P Valat, *J. Lumin.* **75**, 35 (1997)
[10] J C Ronfard-Haret and J Kossanyi, *Chem. Phys.* **241**, 339 (1999)
[11] J S Bae, S B Kim, J H Jeong, J C Park, D K Kim, S H Byeon and S S Yi, *Thin Solid Films* **471**, 225 (2005)
[12] M Morita, D Rau, H Fujii, Y Minami, S Murakami, M Baba, M Yoshita and H Akiyama, *J. Lumin.* **87–89**, 478 (2000)
[13] A A Bol, R van Beek and A Maijerink, *Chem. Mater.* **14**, 1121 (2002)
[14] T Uchihara, H Kato and E Miyagi, *J. Photochem. Photobiol. A: Chem.* **181**, 86 (2006)
[15] A I Savchuk, V I Fediv, A G Voloshchuk, T A Savchuk, Yu Yu Bacherikov and A Perrone, *Mater. Sci. Eng.* **C26**, 809 (2006)
[16] D-W Deng, J-S Yu and Y Pan, *J. Colloid Interface Sci.* **299**, 225 (2006)
[17] A Chahbouna, A G Roloa, S A Filonovicha and M J M Gomes, *Solar Energy Materials & Solar Cells* **90**, 1413 (2006)
[18] C Cheng, G Xu, H Zhang, H Wang, J Cao and H Ji, *Mater. Chem. Phys.* **97**, 448 (2006)
[19] R S Ningthoujam, V Sudarsan and S K Kulshreshtha, *J. Lumin.* **127**, 747 (2007)
[20] G Zhu, K D-Tomsia, H Yu, H Y Motlan and E M Goldys, *Solid State Commun.* **137**, 503 (2006)
[21] G Karve, B Bihari and R T Chen, *Appl. Phys. Lett.* **14**, 1253 (2000)
[22] D An, Z Yue and R T Chen, *Appl. Phys. Lett.* **72**, 2806 (1998)
[23] S Lin, J Feuerstein and A R Mickelson, *J. Appl. Phys.* **79**, 2868 (1996)
[24] M Fuentes, C Mateo, A Rodriguez, M Casqueiro, J C Tercero, H H Riese, R Fernandez-Lafuente and J M Guisan, *Biosensors and Bioelectronics* **21**, 1574 (2006)
[25] L Yang, Q Shen, J Zhou and K Jiang, *Mater. Chem. Phys.* **98**, 125 (2006)